

# A Water-Soluble, AIE-Active Polyelectrolyte for Conventional and Fluorescence Lifetime Imaging of Mouse Neuroblastoma Neuro-2A Cells

Yinan Wang,<sup>1</sup> Hongming Yao,<sup>1</sup> Jian Zhou ,<sup>1</sup> Yuning Hong,<sup>2</sup> Bin Chen,<sup>3</sup> Bolong Zhang,<sup>4</sup> Trevor A. Smith,<sup>4</sup> Wallace W. H. Wong,<sup>4</sup> Zujin Zhao<sup>3</sup>

<sup>1</sup>College of Material, Chemistry and Chemical Engineering, Hangzhou Normal University, Hangzhou 310036, People's Republic of China

<sup>2</sup>Department of Chemistry and Physics, La Trobe University, Victoria 3086, Australia

<sup>3</sup>State Key Laboratory of Luminescent Materials and Devices, South China University of Technology, Guangzhou 510640, People's Republic of China

<sup>4</sup>School of Chemistry, The University of Melbourne, Victoria 3010, Australia

Correspondence to: J. Zhou (E-mail: zhoujian@hznu.edu.cn) or T. A. Smith (E-mail: trevoras@unimelb.edu.au) or Z. Zhao (E-mail: mszjzhao@scut.edu.cn)

Received 22 October 2017; accepted 14 December 2017; published online 00 Month 2018

DOI: 10.1002/pola.28943

**ABSTRACT:** A new conjugated polyelectrolyte containing tetraphenylethene units in the backbone is synthesized and characterized. This polyelectrolyte is water-soluble and exhibits aggregation-induced emission (AIE) behavior. It is biocompatible and can be directly used in conventional and fluorescence lifetime imaging of mouse neuroblastoma neuro-2A cells, providing useful information of cellular morphology and

intracellular aggregation or motion. © 2018 Wiley Periodicals, Inc. *J. Polym. Sci., Part A: Polym. Chem.* **2018**, *00*, 000–000

**KEYWORDS:** aggregation-induced emission; cellular morphology; conjugated polyelectrolyte; fluorescence lifetime imaging; water-soluble

**INTRODUCTION** Conjugated polyelectrolytes (CPEs) comprised of  $\pi$ -electron delocalized backbones and water-soluble side chains have demonstrated great potential applications in chemical and biological sensing<sup>1,2</sup> of various analytes including proteins,<sup>3–5</sup> enzymes,<sup>6–8</sup> DNA,<sup>9,10</sup> and metal ions.<sup>11,12</sup> Owing to their prominent properties, such as high photobleaching resistance, excellent aqueous stability and good biocompatibility, CPEs have been further explored as promising light-activated cellular probes for bioimaging.<sup>13–15</sup> By taking advantage of the electrostatic interaction between CPEs and oppositely charged cells, fluorescent CPEs can easily enter cells for long-term tracking of activities in cells, such as apoptotic process,<sup>16</sup> or generate reactive oxygen species to kill cancer cells.<sup>17–19</sup> However, on account of their inherently amphiphilic structures (hydrophobic backbone and hydrophilic side groups), CPEs have a strong tendency to aggregate in aqueous solution or polar organic solvents, and as a result when they tag proteins within the cells and aggregate strongly, their fluorescence intensity decreases and the emission peak appears as a broad, structureless band, which is red-shifted significantly from its original position in good solvents.<sup>20</sup> Furthermore, compared with the quenching effect for a monomeric model small molecule, CPEs show

considerably larger quenching effect, suggesting that the quenching response is amplified in the polymers.<sup>21</sup> Therefore, traditional CPE-based fluorescent cellular probes mainly operate in a “turn-off” mode. To alleviate the aggregation-caused quenching effect, the CPEs with a hyperbranched architecture, which can self-assemble to form core-shell nanoparticles in aqueous media, have been studied in recent years. These nanoparticles possess well-controlled size and display higher photostability for efficient bioconjugation and specific cellular imaging.<sup>13,22,23</sup>

In recent decades, a novel class of fluorogenic molecules with aggregation-induced emission (AIE) characteristics has sparked enthusiastic research in the design and synthesis of probes for bioimaging applications.<sup>24,25</sup> AIE fluorogens (AIEgens) are nearly non-emissive in the molecularly dispersed state, however, upon aggregating, intramolecular rotation of aromatic rings is restricted and the non-radiative decay channel is blocked, allowing molecules to emit strong fluorescence. Compared with conventional dyes, AIEgens show merits of high brightness, low background signal and good photostability. These superior features enable AIEgens to function as efficient probes in real-time, on-site, and non-

Additional Supporting Information may be found in the online version of this article.

© 2018 Wiley Periodicals, Inc.

invasive visualization of biological molecules, live cells and organisms.<sup>26–30</sup> Whereas noteworthy advances have been achieved regarding small molecular AIE probes, macromolecular AIE probes have been less explored. Macromolecular AIE probes succeed in maintaining many CPE merits including superb physical stability, flexible synthesis, long-term cell tracking, photobleaching resistance, etc.<sup>31–34</sup>

Most fluorescence measurements in cells and tissues are normally made by monitoring relative emission intensity using calibration standards or by self-referencing. Unlike fluorescence intensity-based measurements, time-resolved fluorescence imaging is less affected by experimental conditions such as scattered light or fluorophore concentration.<sup>35,36</sup> Fluorescence lifetimes can be sensitive to a great variety of internal factors defined by the fluorophore structure and external factors including temperature, polarity, viscosity, and the presence of fluorescence quenchers. A combination of environmental sensitivity and parametric independence aforementioned renders time-resolved fluorescence measurements a separate yet complementary method to traditional fluorescence intensity measurements.<sup>37</sup> Therefore, fluorescence lifetime-based spectroscopy or microscopy techniques have already been applied in measurements of graphene quantum dots,<sup>38</sup> light-emitting conjugated polymeric films,<sup>39</sup> the kinetics of  $\alpha$ -chymotrypsin hydrolyzing,<sup>40</sup> imaging of molecular probes in cells, and so forth.<sup>36,41,42</sup> The first work in which living cells stained with AIE small molecules have been imaged using the fluorescence lifetime-based measurement, and provided intracellular viscosity sensing.<sup>43</sup>

In this work, to combine the merits of CPEs and AIEgens, we directly copolymerized a tetraphenylethene (TPE)-based AIEgen with a thiophene-based monomer containing a hydrophilic ether linkage to afford a water-soluble linear CPE with AIE groups in the backbone. TPE-based copolymers normally present an AIE feature, and are considered as suitable candidates for applications in the polymer light-emitting diodes, cell imaging, explosive chemosensors, and so on.<sup>44–50</sup> Similar as these TPE-based copolymers, the new fluorescent CPE also displays AIE characteristics with green emission. The utility as a bioprobe for detection of mouse neuroblastoma neuro-2A cells is investigated through Confocal Laser Scanning Microscopy (CLSM)- and Time Correlated Single Photon Counting (TCSPC)-based fluorescence lifetime imaging (FLIM). This macromolecular AIE bioprobe can enter living cells in a non-invasive manner, and emit bright fluorescence with low cytotoxicity. The fluorescence lifetime-based microscopy based on this probe provides a full map of cellular morphology and molecular motion under various experimental conditions.

## EXPERIMENTAL

### Material and Instruments

4,4'-Dibromobenzophenone, 4,4'-dihydroxybenzophenone, 1,6-dibromohexane, bis-(pinacolato)diborane, 2-(3-thienyl)ethanol, 2-(2-(2-methoxyethoxy)ethoxy)ethyl 4-methylbenzenesulfonate, titanium (IV) chloride, [Pd(dppf)Cl<sub>2</sub>] (dppf = 1,1'-bis(diphenylphosphanyl)ferrocene), Pd(PPh<sub>3</sub>)<sub>4</sub>, potassium t-butoxide,

N-bromosuccinimide, trimethylamine ethanol solution, toluene, *N,N*-dimethylformamide, petroleum spirits, diethyl ether, isopropanol, hexane, acetone, dichloromethane, dioxane, methanol, acetic acid, anhydrous MgSO<sub>4</sub>, KOAc, K<sub>2</sub>CO<sub>3</sub>, KI, zinc dust, SiO<sub>2</sub>, sodium dodecyl sulfate (SDS), hydrochloric acid were purchased from J&K Scientific Ltd., 3-(4,5-dimethyl-2-thiazolyl)-2,5-diphenyltetrazolium bromide (MTT), fetal bovine serum (FBS), penicillin, streptomycin, phosphate-buffered saline (PBS) were purchased from Sigma-Aldrich Company Ltd., and used as received without further purification. THF was purchased from J&K Scientific Ltd., and distilled from sodium benzophenone ketyl under dry nitrogen immediately prior to use. Mouse neuroblastoma neuro-2A cells were obtained from the Bio21 institute (Australia). <sup>1</sup>H and <sup>13</sup>C NMR spectra of small-molecules were measured on a Bruker AV 500 spectrometer in deuterated chloroform using tetramethylsilane (TMS;  $\delta = 0$ ) as the internal reference. <sup>1</sup>H NMR spectra of polymer P1 were measured on an Agilent MR 400 spectrometer in deuterated chloroform using TMS as the internal reference. <sup>13</sup>C NMR spectra of polymer P1 were measured on an Agilent 500 spectrometer in deuterated chloroform using TMS as the internal reference. <sup>1</sup>H NMR spectra of polyelectrolyte P1<sup>+</sup> spectra were measured on an Agilent MR 400 spectrometer in deuterated DMSO using TMS as the internal reference. <sup>13</sup>C NMR spectra of polyelectrolyte P1<sup>+</sup> were measured on an Agilent 500 spectrometer in deuterated DMSO using TMS as the internal reference. UV-vis absorption spectra were measured on a Shimadzu UV-2600 spectrophotometer. Photoluminescence was recorded on a Perkin-Elmer LS 55 spectrofluorometer. Fluorescent decay data were acquired using a Hamamatsu time-resolved spectrometer C11367-11 Quanta-Tau. Mass spectra were recorded on an Agilent 1290 Infinity LC/6530 Q-TOF MS. The number average ( $M_n$ ) and weight average ( $M_w$ ) molecular weights and polydispersity indices (PDI or  $M_w/M_n$ ) of the polymers were estimated by a Waters Associates gel permeation chromatography (GPC 2414) system equipped with RI and UV detectors. Aggregated particle morphologies of polymer were measured by a Hitachi HT-7700 transmission electron microscope (TEM) operated at 80 kV. Average particle size and polydispersities (PDI) of particles were measured by dynamic light scattering (DLS, Zetasizer Nanoseries) at 25 °C under a scattering angle of 90°. Particle sizes were given as the average of three measurements. FLIM images were acquired on a TCSPC-based system (Becker & Hickl, SPC150, Olympus IX71/FV300 confocal microscope using the frequency doubled output (380 nm) of a mode-locked and cavity dumped Titanium: sapphire laser, as described in detail elsewhere<sup>51</sup>), and CLSM images were obtained on a confocal microscope (Leica SP5, Germany) using the LAS AF imaging software.

### Synthesis

#### 4,4'-(2,2-Bis(4-Bromophenyl)Ethene-1,1-Diyl)Diphenol (3)

To a mixture of 4,4'-dibromobenzophenone (3.4 g, 10 mmol), 4,4'-dihydroxybenzophenone (2.14 g, 10 mmol), zinc dust (15.69 g, 0.24 mol) in 80 mL dry THF was added dropwise titanium (IV) chloride (4.55 g, 24 mmol) under N<sub>2</sub> at –78 °C. After stirring for 20 min, the reaction mixture was warmed to room temperature and then heated to reflux for

3.5 h. The mixture was cooled to room temperature and poured into water, and extracted with dichloromethane by three times. The combined organic layers were washed with saturated brine solution and water, and dried over anhydrous  $\text{MgSO}_4$ . After filtration and solvent evaporation, the residue was purified by silica-gel column chromatography using hexane/dichloromethane (2:1) as eluent. White solid of **3** was obtained in 59% yield.  $^1\text{H}$  NMR (400 MHz, DMSO),  $\delta$  (TMS, ppm): 9.38 (s, 2H), 7.31 (d,  $J = 8.4$  Hz, 4H), 6.84 (d,  $J = 8.4$  Hz, 4H), 6.72 (d,  $J = 8.5$  Hz, 4H), 6.51 (d,  $J = 8.5$  Hz, 4H).  $^{13}\text{C}$  NMR (100 MHz, DMSO),  $\delta$  (TMS, ppm): 156.7, 143.44, 142.52, 135.54, 133.92, 133.37, 132.49, 131.28, 119.73, 115.2. HRMS:  $m/z$  522.9729 ( $[\text{M} + \text{H}]^+$ , calcd for  $\text{C}_{26}\text{H}_{19}\text{Br}_2\text{O}_2$  522.9731).

#### 4,4'-(2,2-Bis(4-((6-Bromohexyl)Oxy)Phenyl)Ethene-1,1-Diyl)Bis(Bromobenzene) (**4**)

To a mixture of **3** (2.09 g, 4 mmol), 1,6-dibromohexane (4.88 g, 20 mmol),  $\text{K}_2\text{CO}_3$  (2.76 g, 20 mmol), and KI (33.2 mg, 0.2 mmol) in 30 mL acetone. The reaction mixture was heated to reflux for 12 h. The mixture was cooled to room temperature and poured into water, and extracted with dichloromethane by three times. The combined organic layers were washed with saturated brine solution and water, and dried over anhydrous  $\text{MgSO}_4$ . After filtration and solvent evaporation, the residue was purified by silica-gel column chromatography using hexane/dichloromethane (2:1) as eluent. White solid of **4** was obtained in 44% yield.  $^1\text{H}$  NMR (400 MHz,  $\text{CDCl}_3$ ),  $\delta$  (TMS, ppm): 7.22 (d,  $J = 8.4$  Hz, 4H), 6.87 (dd, 8H), 6.63 (d,  $J = 8.6$  Hz, 4H), 3.90 (t,  $J = 6.4$  Hz, 4H), 3.42 (t,  $J = 6.8$  Hz, 4H), 1.93–1.85 (m, 4H), 1.80–1.73 (m, 4H), 1.53–1.45 (m, 8H).  $^{13}\text{C}$  NMR (100 MHz,  $\text{CDCl}_3$ ),  $\delta$  (TMS, ppm): 157.88, 142.81, 141.55, 135.46, 132.98, 132.48, 130.96, 120.21, 113.70, 67.55, 33.79, 32.65, 29.09, 27.92, 25.30. HRMS:  $m/z$  847.9705 ( $\text{M}^+$ , calcd for  $\text{C}_{38}\text{H}_{40}\text{Br}_4\text{O}_2$  847.9721).

#### 2,2'-((2,2-Bis(4-((6-Bromohexyl)Oxy)Phenyl)Ethene-1,1-Diyl)Bis(4,1-Phenylene))Bis(4,4,5,5-Tetramethyl-1,3,2-Dioxaborolane) (**5**)

**4** (8.48g, 10 mmol), bis-(pinacolato)diborane (6.10 g, 24 mmol), KOAc (6.87 g, 70 mmol), and dioxane (100 mL) were mixed together in a 250 mL flask. After degassing,  $[\text{Pd}(\text{dppf})\text{Cl}_2]$  (0.8 g,  $\text{dppf} = 1,1'$ -bis(diphenylphosphanyl)ferrocene) was added. The reaction mixture was kept at 95 °C overnight, and then cooled to room temperature. The organic solvent was distilled out, and the residual solid was dissolved in dichloromethane and washed with water. After drying with anhydrous  $\text{MgSO}_4$ , the solvent was distilled out. The crude product was purified by flash chromatography using hexanes and dichloromethane (1:1) as the eluent and then recrystallized in isopropanol to give **5** as white crystals (5.56 g, 59%).  $^1\text{H}$  NMR (400 MHz,  $\text{CDCl}_3$ ),  $\delta$  (TMS, ppm): 7.52 (d,  $J = 7.9$  Hz, 4H), 7.00 (d,  $J = 7.9$  Hz, 4H), 6.90 (d,  $J = 8.6$  Hz, 4H), 6.60 (d,  $J = 8.6$  Hz, 4H), 3.88 (t,  $J = 6.4$  Hz, 4H), 3.42 (t,  $J = 6.8$  Hz, 4H), 1.92–1.86 (m, 4H), 1.79–1.73 (m, 4H), 1.52–1.46 (m, 8H), 1.32 (s, 24H).  $^{13}\text{C}$  NMR (100 MHz,  $\text{CDCl}_3$ ),  $\delta$  (TMS, ppm): 157.66, 147.25, 141.21, 138.83,

136.02, 134.07, 132.58, 130.80, 113.52, 83.64, 67.43, 33.80, 32.68, 29.12, 27.95, 25.33, 24.88. HRMS:  $m/z$  943.3314 ( $[\text{M} + \text{H}]^+$ , calcd for  $\text{C}_{50}\text{H}_{65}\text{B}_2\text{Br}_2\text{O}_6$  943.3314).

#### 13-(Thiophen-3-yl)-2,5,8,11-Tetraoxatridecane (**8**)

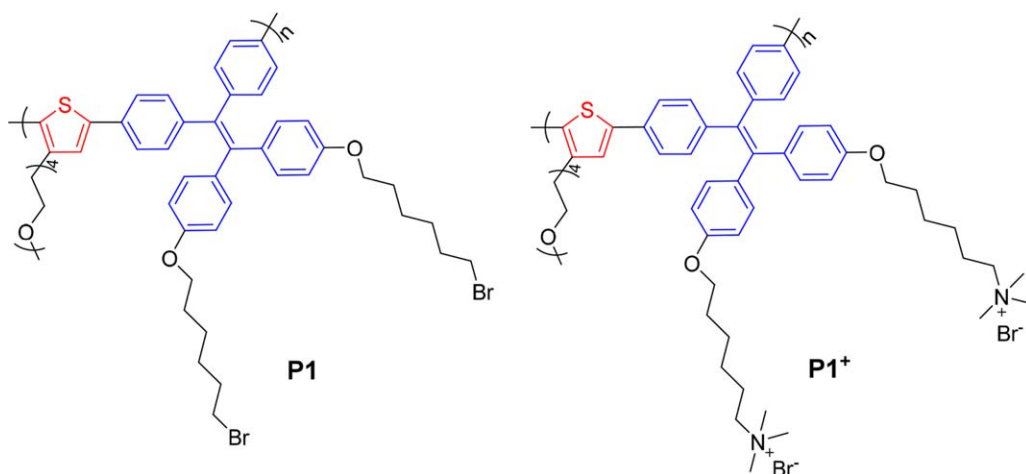
**8** was synthesized using methods reported in the literature.<sup>52</sup>

#### 13-(2,5-Dibromothiophen-3-yl)-2,5,8,11-Tetraoxatridecane (**9**)

Thiophene **8** (200 mg, 0.73 mmol) was dissolved in acetic acid (1 mL). *N*-Bromosuccinimide (285 mg, 1.60 mmol) was added portionwise and the reaction was stirred at 25 °C for 14 h. Water was added to the reaction and the organic material was extracted with petroleum spirits 40–60 °C. Pure product **9** was isolated after  $\text{SiO}_2$  column chromatography purification (petroleum spirits 40–60 °C/diethyl ether).  $^1\text{H}$  NMR (400 MHz,  $\text{CDCl}_3$ ),  $\delta$  (TMS, ppm): 6.88 (s, H), 3.65–3.59 (m, 12H), 3.55–3.52 (m, 2H), 3.37 (s, 3H), 2.8 (t,  $J = 6.8$  Hz, 2H).  $^{13}\text{C}$  NMR (101 MHz,  $\text{CDCl}_3$ ),  $\delta$  (TMS, ppm): 139.54, 131.47, 110.35, 108.95, 71.92, 70.63, 70.56, 70.51, 70.27, 69.87, 59.03, 29.93. HRMS:  $m/z$  432.9502 ( $[\text{M} + \text{H}]^+$ , calcd for  $\text{C}_{13}\text{H}_{21}\text{Br}_2\text{O}_4\text{S}$  432.9507).

**P1**: To a mixture of **5** (235 mg, 0.25 mmol), **9** (108 mg, 0.25 mmol),  $\text{Pd}(\text{PPh}_3)_4$  (12 mg, 0.01 mmol), and  $\text{K}_2\text{CO}_3$  (276 mg, 2 mmol) in a 10 mL round-bottomed flask. A mixture of toluene (1 mL) and water (1 mL) was added to the flask, and the reaction vessel was degassed. The mixture was vigorously stirred at 85 °C for 24 h and then cooled to room temperature. After extraction with dichloromethane, the combined organic layers were washed successively with water and then dried over anhydrous  $\text{MgSO}_4$ . The polymer was filtered and precipitated into methanol, and then dried under vacuum for 24 h to afford the neutral polymer P1 as a green solid in 68% yield.  $^1\text{H}$  NMR (400 MHz,  $\text{CDCl}_3$ ),  $\delta$  (TMS, ppm): 7.36–7.32 (m, 2H), 7.24–7.21 (m, 2H), 7.19 (s, H), 7.09–7.02 (m, 4H), 6.95 (d,  $J = 6.9$  Hz, 4H), 6.64 (d,  $J = 7.9$ , 4H), 3.89 (t,  $J = 5.8$  Hz, 4H), 3.70–3.56 (m, 14H), 3.51–3.49 (m, 2H), 3.40 (t,  $J = 6.7$  Hz, 4H), 3.34 (s, 3H), 1.92–1.82 (m, 4H), 1.79–1.72 (m, 4H), 1.52–1.41 (m, 8H).  $^{13}\text{C}$  NMR (100 MHz,  $\text{CDCl}_3$ ),  $\delta$  (TMS, ppm): 157.70, 143.36, 141.86, 140.91, 138.42, 137.93, 136.13, 135.42, 132.65, 131.96, 131.66, 128.27, 125.66, 124.59, 113.60, 71.90, 71.40, 70.60, 70.48, 70.30, 67.52, 59.01, 33.80, 32.66, 29.11, 27.94, 25.31.

**P1**<sup>+</sup>: Condensed trimethylamine ethanol solution (2 mL, 2.4 M) was added drop-wise to a solution of the neutral polymer P1 (50 mg) in THF (10 mL) at 0 °C. The mixture was allowed to warm to room temperature. The precipitate was redissolved by the addition of water (10 mL). After the mixture was cooled to 0 °C, additional trimethylamine ethanol solution (2 mL, 2.4 M) was added, and the mixture was stirred at room temperature for 24 h. After removal of the solvent, acetone was added to precipitate the CPEs as deep green powder in 80% yield for P1<sup>+</sup>.  $^1\text{H}$  NMR (400 MHz, DMSO),  $\delta$  (TMS, ppm): 7.48–7.24 (m, 5H), 7.08–6.94 (m, 4H), 6.92–6.81 (br, 4H), 6.74–6.64 (br, 4H), 3.87 (br, 4H), 3.66–3.38 (m, 16H), 3.36–3.21 (br, 4H), 3.16 (s, 3H), 3.03 (s, 18H), 1.73–1.60 (br, 8H), 1.46–1.25 (m, 8H).  $^{13}\text{C}$  NMR (100 MHz,

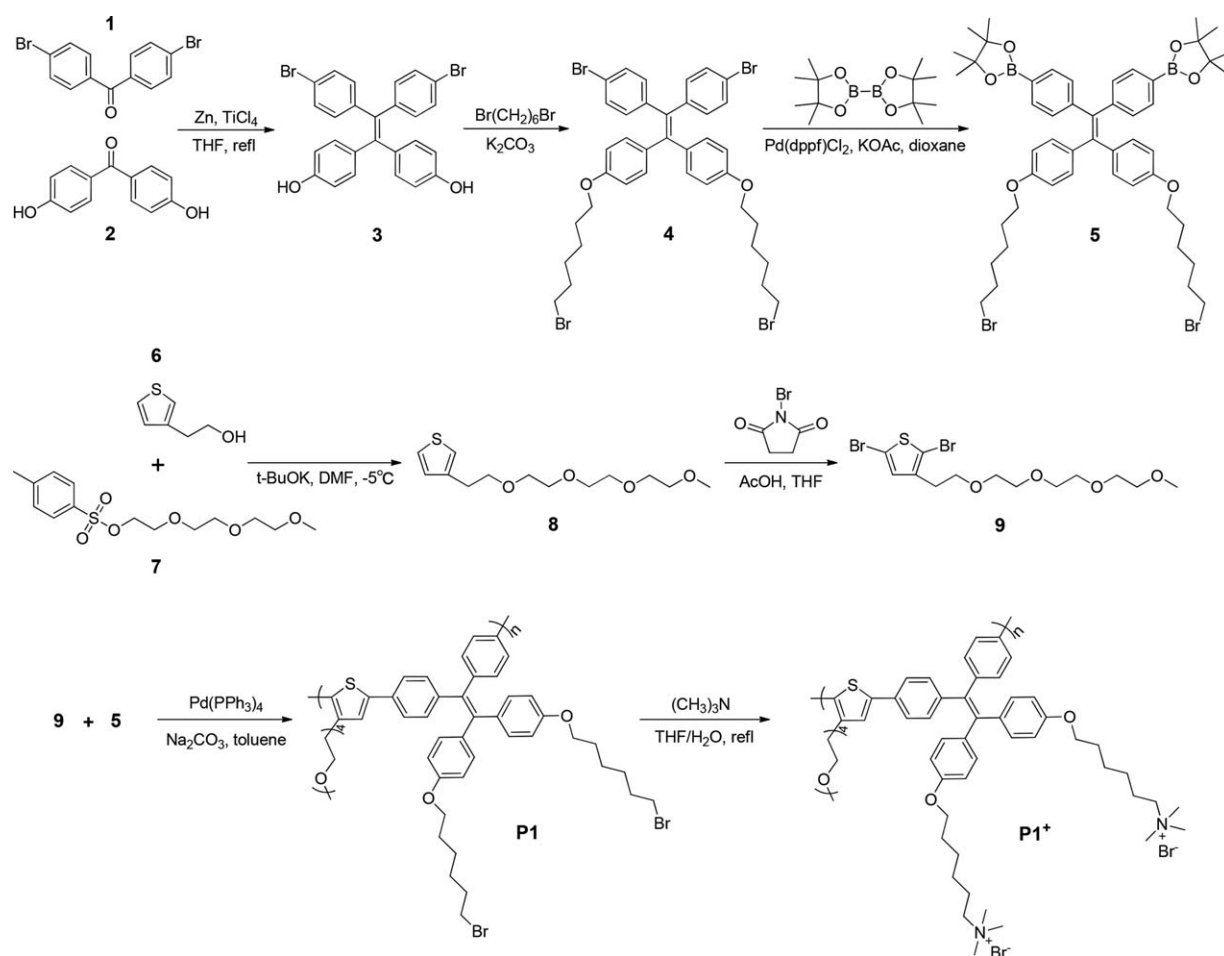


**SCHEME 1** Molecular structures of 4,4'-(2,2-diphenylethene-1,1-diyl)bis((alkyloxy)benzene)-based copolymers P1 and P1<sup>+</sup>. [Color figure can be viewed at [wileyonlinelibrary.com](http://wileyonlinelibrary.com)]

DMSO),  $\delta$  (TMS, ppm): 157.80, 143.49, 141.06, 137.63, 136.76, 135.91, 132.54, 132.00, 131.73, 128.60, 127.13, 124.85, 114.17, 71.69, 70.55, 70.24, 70.00, 67.58, 65.62, 58.47, 52.57, 28.91, 25.94, 25.54, 22.42.

### Cell Culture and Fluorescence Imaging

The mouse neuroblastoma neuro-2A cells were cultured in minimum essential medium (MEM) containing 10% FBS, 100 U mL<sup>-1</sup> penicillin, and 100  $\mu$ g mL<sup>-1</sup> streptomycin in a 5%



**SCHEME 2** Synthetic routes to 4,4'-(2,2-diphenylethene-1,1-diyl)bis((alkyloxy)benzene)-based copolymers.

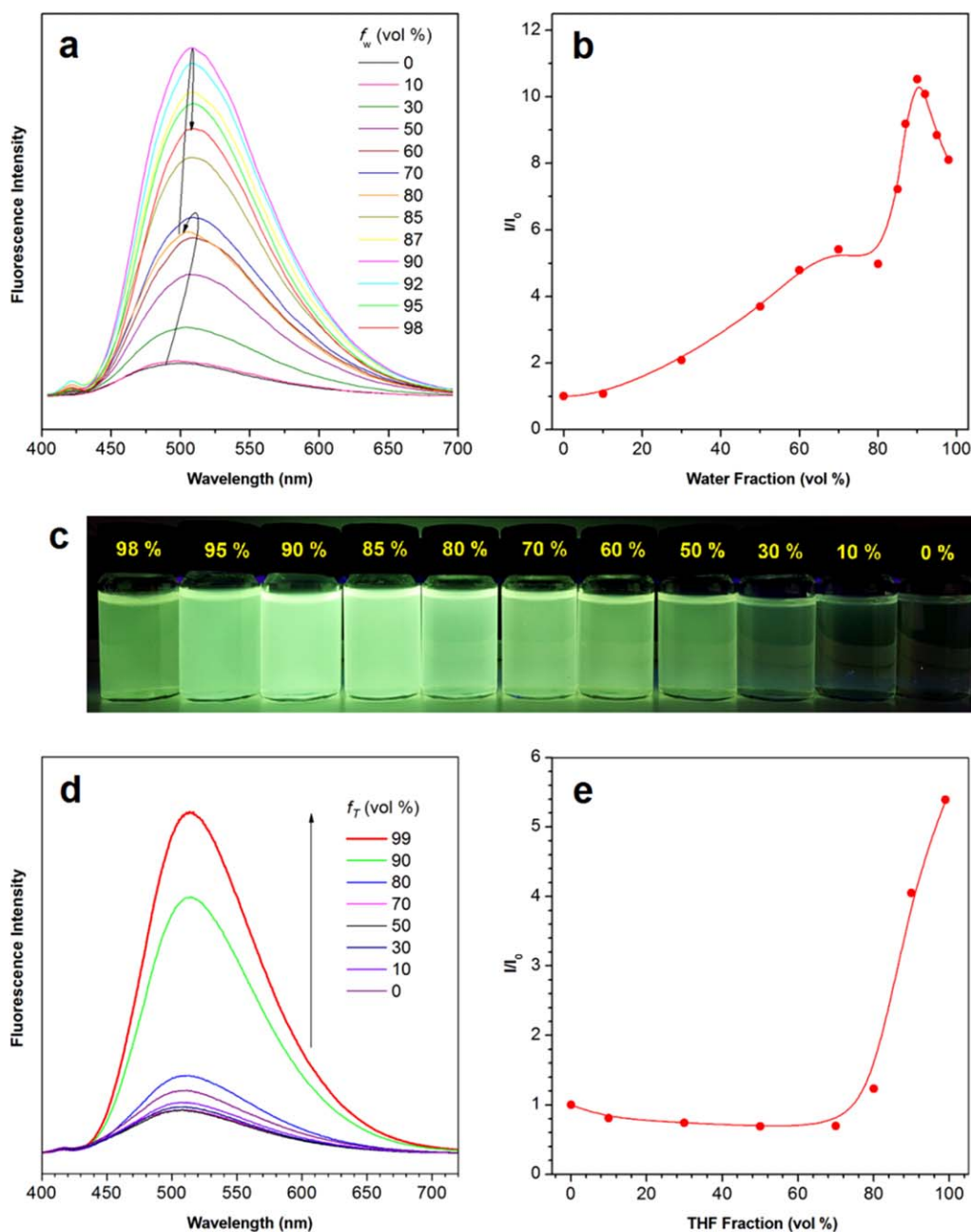


**FIGURE 1** (a) Fluorescence emission spectra of P1 in Water-THF mixtures with different water fractions. (b) Plot of relative PL intensity ( $I/I_0$ ) versus the composition of the aqueous mixture of P1. (c) Photographs of P1 in THF solution and water-THF mixtures (water volume fraction from 0% to 98%) taken under UV lamp illumination. (d) Fluorescence emission spectra of polyelectrolyte  $P1^+$  in DMSO solution and DMSO-THF mixture. (e) Plot of relative PL intensity ( $I/I_0$ ) versus the composition of DMSO-THF mixture of polyelectrolyte  $P1^+$ . Solution concentration:  $10 \mu\text{M}$ ; excitation wavelength: 370 nm. [Color figure can be viewed at wileyonlinelibrary.com]

$\text{CO}_2$  humidity incubator at  $37^\circ\text{C}$ . The mouse neuroblastoma neuro-2A cells were grown in a 35 mm Petri dish with a coverslip at  $37^\circ\text{C}$ . The living cells were stained with  $P1^+$  ( $5 \mu\text{g mL}^{-1}$  or  $20 \mu\text{g mL}^{-1}$ ) for 30 min. The cells were washed for three times with PBS buffer and imaged under CLSM.  $P1^+$  was excited at 405 nm and the fluorescence was collected at 450–650 nm. The cells were further imaged by FLIM. The excitation wavelength is 400 nm for  $P1^+$ . The

emission was collected through a  $500 \pm 15$  nm band pass filter for  $P1^+$ .

Cell Viability Evaluated by MTT Assay: Viability of the cells was assayed by using cell proliferation Kit I with the absorbance of 595 nm being detected using a Perkin-Elmer Victor plate reader. Five thousand cells were seeded per well in a 96-well plate. After overnight culture,  $P1^+$  with various

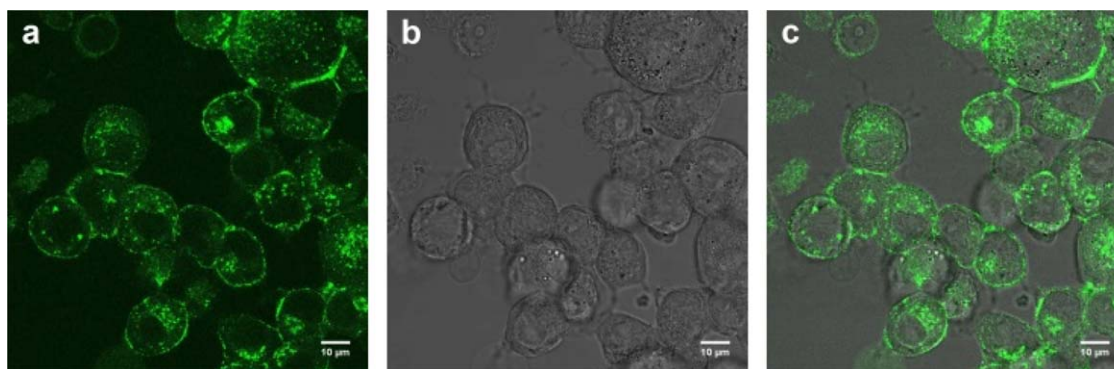


**FIGURE 2** Fluorescent images of mouse neuroblastoma neuro-2A cells stained with  $P1^+$  ( $5 \mu\text{g mL}^{-1}$ ) for 0.5 h at  $37^\circ\text{C}$ . (a) fluorescence image, (b) bright field image, and (c) the overlay of fluorescence image and bright field image. [Color figure can be viewed at [wileyonlinelibrary.com](http://wileyonlinelibrary.com)]

concentrations was added into the 96-well plate. After 2 h treatment,  $10 \mu\text{L}$  of MTT solution ( $5 \text{ mg mL}^{-1}$  in PBS) was added into the each well. After 4 h incubation at  $37^\circ\text{C}$ ,  $100 \mu\text{L}$  of solubilization solution containing 10% SDS and 0.01 M HCl was added to dissolve the purple crystals. After 12 h incubation, the optical density readings at 595 nm were taken using a plate reader. Each of the experiments was performed at least 3 times.<sup>53</sup>

## RESULTS AND DISCUSSION

### Synthesis of Polymer

Scheme 1 illustrates the molecular structure of the neutral polymer (P1) and CPE ( $P1^+$ ). P1 is synthesized by Suzuki coupling of 4,4'-(2,2-bis(4-((6-bromohexyl)oxy)phenyl)ethene-1,1-diyl)bis(bromobenzene) with 1,3-(2,5-dibromothiophen-3-yl)-2,5,8,11-tetraoxatridecane in 68% yield. P1 is then reacted with trimethylamine to yield the cationic conjugated polymer  $P1^+$  (Scheme 2). The detailed synthetic procedures and characterization data are given in the experimental section. The GPC analysis shows that the weight-average molecular weight ( $M_w$ ) of P1 is  $48,337 \text{ g mol}^{-1}$  and the polydispersity is 2.28 (Fig. S1, Supporting Information). The presence of flexible *n*-octyl groups should have ameliorated the solubility of the polymer, which reduces the precipitation in the reaction process, and thus, enhances the molecular weight of the polymer. Although the molecular weight is high,  $P1^+$  possesses water solubility owing to the hydrophilic long chain ether groups on the thiophene units and the quaternary ammonium salt groups on the TPE units.

### Photophysical Properties of Polymer

The absorption maximum of P1 is located at 367 nm (Fig. S2, Supporting Information). P1 displays typical AIE characteristics, similar to previously reported TPE-containing polymers.<sup>54,55</sup> As shown in Figure 1(a–c), P1 possesses a good solubility in THF and shows weak emission at 498 nm with a fluorescence quantum yield ( $\Phi_F$ ) of 1.4% in THF. This is because its phenyl rings of the TPE moieties undergo active intramolecular rotations in THF, which nonradiatively annihilates its excited state and makes it almost nonemissive.<sup>56–58</sup>

However, with gradual addition of water, a poor solvent for P1, into THF, the resultant THF–water mixtures exhibit significantly enhanced emission with an increased  $\Phi_F$  of 24.4% at a water fraction of 90 vol %. In solid film, P1 also gives a high  $\Phi_F$  of 24.5%. The increase in  $\Phi_F$  in both the THF/water mixture and the film is attributed to the hindrance of intramolecular rotation within P1, likely due to aggregation in the case of the solvent mixture and to either aggregation and/or the rotationally restricted environment within the film. This restriction of the intramolecular rotation (RIR) blocks the nonradiative decay channel, thus making the aggregates highly fluorescent. Therefore, the P1 indeed exhibits AIE properties.<sup>57,58</sup> The maximal emission peak at 508 nm is red-shifted by 10 nm when compared with that in solution, which is probably attributable to intermolecular interactions in the aggregate state.<sup>59</sup> The fluorescence decay profiles of P1 in THF and the THF/water mixture were not exponential (Fig. S3, Supporting Information) but average lifetimes ( $\tau_{AVE}$ ) were computed, as per the equation  $\tau_{AVE} = \sum f_i \tau_i$ ,

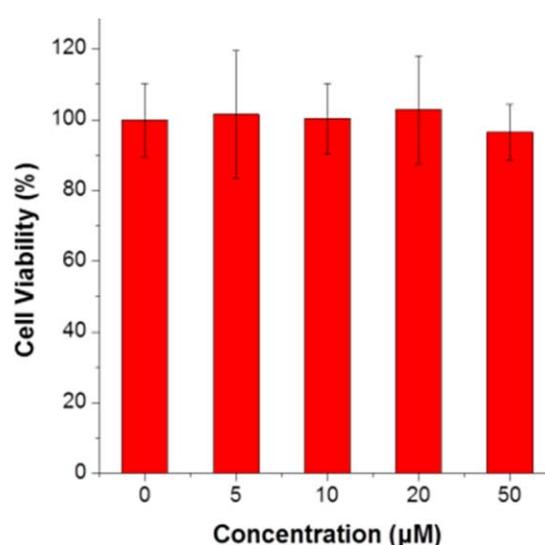


**FIGURE 3** Cytotoxicity of  $P1^+$  on neuro-2A cells determined by MTT assay. [Color figure can be viewed at [wileyonlinelibrary.com](http://wileyonlinelibrary.com)]

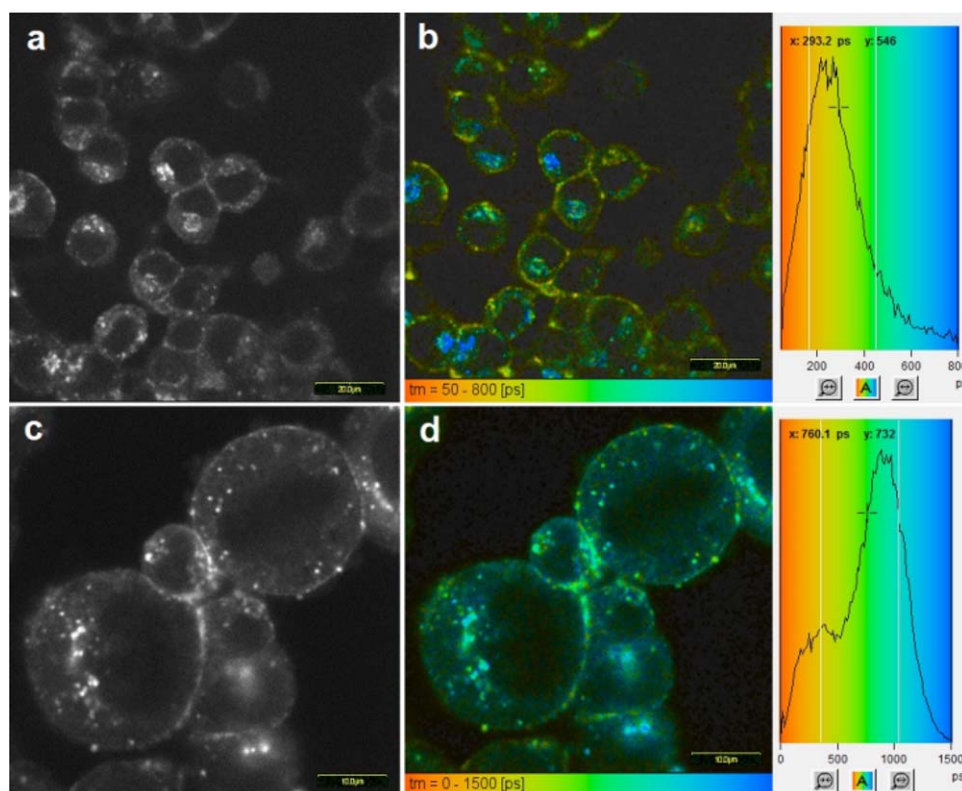


**FIGURE 4** Fluorescence lifetime images of mouse neuroblastoma neuro-2A cells stained with  $P1^+$  ( $5 \mu\text{g mL}^{-1}$  for a and b;  $20 \mu\text{g mL}^{-1}$  for c and d) for 0.5 h at  $37^\circ\text{C}$ . [Color figure can be viewed at [wileyonlinelibrary.com](http://wileyonlinelibrary.com)]

(where  $f_i$  is the fractional contribution of the individual lifetime of each component ( $\tau_i$ )).<sup>60</sup> The  $\tau_{\text{AVE}}$  is enhanced from 0.189 ns to 1.112 ns with the addition of water into the THF solution from zero to 90 vol % aqueous mixture, which is consistent with the observed changes in emission intensity.

The corresponding conjugated polymer  $P1^+$  also exhibits AIE characteristics.  $P1^+$  shows weak emission in DMSO, however, when a large amount of THF, a poor solvent for the  $P1^+$ , is added to the DMSO solution of  $P1^+$  ( $f_{\text{THF}} > 80$  vol %), strong green emission is observed [Fig. 1(d,e)], and longer lifetime can be detected (Fig. S4, Supporting Information). In the mixture with a high THF fraction,  $P1^+$  has formed aggregates as conformed by TEM and DLS (Fig. S5, Supporting Information). The emission intensity of  $P1^+$  in aqueous solutions is also increased dramatically with the increase in  $P1^+$  concentration [Fig. S6(a), Supporting Information].  $P1$  in the aggregated state not only has relatively stronger fluorescence intensity but also longer fluorescence lifetime. Thus, the large aggregation dependence of the time-resolved fluorescence decay process and  $\Phi_F$  of  $P1^+$  prompt us to explore the possibility of imaging the microstructures inside living cells with the  $P1^+$ , as complementary method to traditional fluorescence intensity measurements.

#### Fluorescent Images of Cells Stained with $P1^+$

$P1^+$  is assessed for its ability to interact with live mouse neuroblastoma neuro-2A cells using a confocal fluorescence microscope. After incubation with  $5 \mu\text{g mL}^{-1}$   $P1^+$  for 30 min,

the profile and microscopic structure of cells are clearly visible and bright green emission is observed (Fig. 2), suggesting  $P1^+$  can enter and stain living cells easily. In particular, some  $P1^+$  molecules are directly endocytosed by the cells and distributed in the cytoplasm, while others stay in the thin cytomembrane, so that the cells' round profile can be distinctly observed. The cytotoxicity of  $P1^+$  was evaluated by the widely used MTT assay. The samples were incubated with 0, 5, 10, 20, and  $50 \mu\text{M}$   $P1^+$  for 24 h, and at the highest concentration of  $50 \mu\text{M}$ , the cell viability remains  $\sim 96\%$ . This result suggests the water-soluble  $P1^+$  has good biocompatibility (Fig. 3).

#### Fluorescence Lifetime Images of Cells Stained with $P1^+$

To further explore the density of  $P1^+$  in the neuro-2A cells, the incubated cells were imaged using FLIM based on a TCSPC system. Owing to the large difference in the time-resolved fluorescent decay process of  $P1$  at different molecular diffusion level, it is reasonable that  $P1^+$  with higher density in the cells can display longer fluorescence lifetime as well. Since the fluorescence lifetime of  $P1^+$  in aqueous solution cannot be continuously enhanced as the increase in concentration [Fig. S6(b,c), Supporting Information], the incubation contents of  $P1^+$  in MEM are set at  $5 \mu\text{g mL}^{-1}$  and  $20 \mu\text{g mL}^{-1}$ , respectively, for comparing the distribution of  $P1^+$  in cells. FLIM images of the neuro-2A cells incubated with  $P1^+$  are shown in Figure 4, by applying a color scale from short (indicated by red color) to long (indicated by

blue color) lifetimes. These images reveal that  $P1^+$  may be utilized as a probe for directly visualizing the cells' morphology, and more importantly, we can observe that the  $P1^+$  remaining in the cytomembrane shows shorter lifetimes while that entering into the cells exhibits longer lifetimes. The lifetime histograms suggest that more  $P1^+$  molecules stay in the cytomembrane rather than entering into the cells under low concentration conditions. Increasing the incubation concentration, leads to more  $P1^+$  molecules being endocytosed by the cells and located inside the cells. The color distribution of the images supports the hypothesis that  $P1^+$  molecules are inclined to aggregate in the central areas of cells rather than the cytomembrane. Long fluorescence lifetime areas in cells indicate the molecular motions slow down, probably due to aggregation or high viscosity in these regions.

## CONCLUSIONS

In this work, we have designed and synthesized a neutral TPE-containing polymer P1, which is quaternized to afford a polyelectrolyte  $P1^+$ .  $P1^+$  possesses water solubility and shows AIE characteristics and strong green emission in the aggregated state.  $P1^+$  is biocompatible and exhibits good performance in labeling mouse neuroblastoma neuro-2A cells as revealed by CLSM- and TCSPC-based FLIM techniques. The results from FLIM images support the hypothesis that  $P1^+$  molecules are inclined to aggregate in the central areas of cells exhibiting longer fluorescence lifetimes, while those staying on the cytomembrane are aggregated loosely associated with shorter fluorescence lifetimes. The molecular motion of  $P1^+$  in cells can be monitored, providing information about aggregation or environmental viscosity as a function of location in cells. As such, we believe that this work could open a new avenue in the field of tracking the cancer cells using AIE CPEs through both the CLSM- and TCSPC-based FLIM technology.

## ACKNOWLEDGMENTS

We acknowledge the financial support from the National Natural Science Foundation of China (21404029, 21344007, and 21673082), the China Scholarship Council (201409645002), the Guangdong Natural Science Funds for Distinguished Young Scholar (2014A030306035), Scientific Research Fund of Zhejiang Provincial Education Department (Y201121319), and the Fundamental Research Funds for the Central Universities (2017ZD001).

## REFERENCES AND NOTES

- 1 X. Duan, L. Liu, F. Feng, S. Wang, *Acc. Chem. Res.* **2010**, *43*, 260.
- 2 A. Duarte, K. Pu, B. Liu, G. C. Bazan, *Chem. Mater.* **2011**, *23*, 501.
- 3 X. Zhu, S. Guo, T. He, S. Jiang, D. Jańczewski, G. J. Vancso, *Langmuir* **2016**, *32*, 1338.
- 4 C. J. Arias, R. L. Surmaitis, J. B. Schlenoff, *Langmuir* **2016**, *32*, 5412.
- 5 J. You, T. Park, J. Kim, J. S. Heo, H. Kim, H. O. Kim, E. Kim, *ACS Appl. Mater. Interfaces* **2014**, *6*, 3305.
- 6 A. K. Dwivedi, P. K. Lyer, *J. Mater. Chem. B* **2013**, *1*, 4005.
- 7 R. Zhan, A. J. H. Tan, B. Liu, *Polym. Chem.* **2011**, *2*, 417.
- 8 R. Liu, Y. Tan, C. Zhang, J. Wu, L. Mei, Y. Jiang, C. Tan, *J. Mater. Chem. B* **2013**, *1*, 1402.
- 9 C. Nie, C. Zhu, L. Feng, F. Lv, L. Liu, S. Wang, *ACS Appl. Mater. Interfaces* **2013**, *5*, 4549.
- 10 G. Yang, H. Yuan, C. Zhu, L. Liu, Q. Yang, F. Lv, S. Wang, *ACS Appl. Mater. Interfaces* **2012**, *4*, 2334.
- 11 J. You, J. Kim, T. Park, B. Kim, E. Kim, *Adv. Funct. Mater.* **2012**, *22*, 1417.
- 12 B. Bao, L. Yuwen, X. Zhan, L. Wang, *J. Polym. Sci. Part A: Polym. Chem.* **2010**, *48*, 3431.
- 13 P. Zhang, H. Lu, H. Chen, J. Zhang, L. Liu, F. Lv, S. Wang, *Anal. Chem.* **2016**, *88*, 2985.
- 14 M. Li, S. Li, H. Chen, R. Hu, L. Liu, F. Lv, S. Wang, *ACS Appl. Mater. Interfaces* **2016**, *8*, 42.
- 15 A. Parthasarathy, H. Ahn, K. D. Belfield, K. S. Schanze, *ACS Appl. Mater. Interfaces* **2010**, *2*, 2744.
- 16 Y. Liu, P. Wu, J. Jiang, J. Wu, Y. Chen, Y. Tan, C. Tan, Y. Jiang, *ACS Appl. Mater. Interfaces* **2016**, *8*, 21984.
- 17 R. Hu, H. Yuan, B. Wang, L. Liu, F. Lv, S. Wang, *ACS Appl. Mater. Interfaces* **2014**, *6*, 11823.
- 18 H. Yuan, H. Chong, B. Wang, C. Zhu, L. Liu, Q. Yang, F. Lv, S. Wang, *J. Am. Chem. Soc.* **2012**, *134*, 13184.
- 19 H. Chong, C. Nie, C. Zhu, Q. Yang, L. Liu, F. Lv, S. Wang, *Langmuir* **2012**, *28*, 2091.
- 20 C. Tan, E. Atas, J. G. Muller, M. R. Pinto, V. D. Kleiman, K. S. Schanze, *J. Am. Chem. Soc.* **2004**, *126*, 13685.
- 21 H. Jiang, P. Taranekekar, J. R. Reynolds, K. S. Schanze, *Angew. Chem. Int. Ed.* **2009**, *48*, 4300.
- 22 K. Pu, K. Li, J. Shi, B. Liu, *Chem. Mater.* **2009**, *21*, 3816.
- 23 K. Pu, J. Shi, L. Cai, K. Li, B. Liu, *Biomacromolecules* **2011**, *12*, 2966.
- 24 Y. Hong, J. W. Y. Lam, B. Z. Tang, *Chem. Commun.* **2009**, 4332.
- 25 J. Mei, N. L. C. Leung, R. T. K. Kwok, J. W. Y. Lam, B. Z. Tang, *Chem. Rev.* **2015**, *115*, 11718.
- 26 J. Liang, B. Z. Tang, B. Liu, *Chem. Soc. Rev.* **2015**, *44*, 2798.
- 27 M. Gao, C. K. Sim, C. W. T. Leung, Q. Hu, G. Feng, F. Xu, B. Z. Tang, B. Liu, *Chem. Commun.* **2014**, *50*, 8312.
- 28 Y. Hong, L. Meng, S. Chen, C. W. T. Leung, L. Da, M. Faisal, D. Silva, J. Liu, J. W. Y. Lam, X. Huang, B. Z. Tang, *J. Am. Chem. Soc.* **2012**, *134*, 1680.
- 29 C. W. T. Leung, Y. Hong, S. Chen, E. Zhao, J. W. Y. Lam, B. Z. Tang, *J. Am. Chem. Soc.* **2013**, *135*, 62.
- 30 Y. Yu, C. Feng, Y. Hong, J. Liu, S. Chen, K. M. Ng, K. Q. Luo, B. Z. Tang, *Adv. Mater.* **2011**, *23*, 3298.
- 31 R. Hu, N. L. C. Leung, B. Z. Tang, *Chem. Soc. Rev.* **2014**, *43*, 4494.
- 32 Z. Wang, S. Chen, J. W. Y. Lam, W. Qin, R. T. K. Kwok, N. Xie, Q. Hu, B. Z. Tang, *J. Am. Chem. Soc.* **2013**, *135*, 8238.
- 33 X. Zhang, X. Zhang, B. Yang, J. Hui, M. Liu, Z. Chi, S. Liu, J. Xu, Y. Wei, *Polym. Chem.* **2014**, *5*, 683.
- 34 H. Lu, F. Su, Q. Mei, Y. Tian, W. Tian, R. H. Johnson, D. R. Meldrum, *J. Mater. Chem.* **2012**, *22*, 9890.
- 35 Y. Chen, A. Periasamy, *Microsc. Res. Tech.* **2004**, *63*, 72.

- 36** P. Sarder, D. Maji, S. Achilefu, *Bioconjug. Chem.* **2015**, *26*, 963.
- 37** M. Y. Berezin, S. Achilefu, *Chem. Rev.* **2010**, *110*, 2641.
- 38** M. Roding, S. J. Bradley, M. Nyden, T. Nann, *J. Phys. Chem. C* **2014**, *118*, 30282.
- 39** X. Hao, L. J. McKimmie, T. A. Smith, *J. Phys. Chem. Lett.* **2011**, *2*, 1520.
- 40** T. G. Terentyeva, J. Hofkens, T. Komatsuzaki, K. Blank, C. Li, *J. Phys. Chem. B* **2013**, *117*, 1252.
- 41** C. M. Roth, P. I. Heinlein, M. Heilemann, D. P. Herten, *Anal. Chem.* **2007**, *79*, 7340.
- 42** E. Derivery, C. Seum, A. Daeden, S. Loubery, L. Holtzer, F. Julicher, M. Gonzalez-Gaitan, *Nature* **2015**, *528*, 280.
- 43** S. Chen, Y. Hong, Y. Zeng, Q. Sun, Y. Liu, E. Zhao, G. Bai, J. Qu, J. Hao, B. Z. Tang, *Chem. Eur. J.* **2015**, *21*, 4315.
- 44** B. He, S. Ye, Y. Guo, B. Chen, X. Xu, H. Qiu, Z. Zhao, *Sci. China Chem.* **2013**, *56*, 1221.
- 45** R. Chen, X. Gao, X. Cheng, A. Qin, J. Z. Sun, B. Z. Tang, *Polym. Chem.* **2017**, *8*, 6277.
- 46** L. He, L. Li, X. Liu, J. Wang, H. Huang, W. Bu, *Polym. Chem.* **2016**, *7*, 3722.
- 47** A. H. Malik, A. Kalita, P. K. Iyer, *ACS Appl. Mater. Interfaces* **2017**, *9*, 37501.
- 48** J. Tu, M. Zhao, X. Zhan, Z. Ruan, H. Zhang, Q. Li, Z. Li, *Polym. Chem.* **2016**, *7*, 4054.
- 49** W. Wu, S. Ye, R. Tang, L. Huang, Q. Li, G. Yu, Y. Liu, J. Qin, Z. Li, *Polymer* **2012**, *53*, 3163.
- 50** W. Wu, S. Ye, G. Yu, Y. Liu, J. Qin, Z. Li, *Macromol. Rapid Commun.* **2012**, *33*, 164.
- 51** J. L. Hickey, J. L. James, C. A. Henderson, K. A. Price, A. I. Mot, G. Buncic, P. J. Crouch, J. M. White, A. R. White, T. A. Smith, P. S. Donnelly, *Inorg. Chem.* **2015**, *54*, 9556.
- 52** B. D. Boer, P. F. V. Hutten, L. Ouali, V. Grayer, G. Hadziioannou, *Macromolecules* **2002**, *35*, 6883.
- 53** M. Gao, Y. Hong, B. Chen, Y. Wang, W. Zhou, W. W. H. Wong, J. Zhou, T. A. Smith, Z. Zhao, *Polym. Chem.* **2017**, *8*, 3862.
- 54** Y. Wu, J. Shi, B. Tong, J. Zhi, Y. Dong, *Acta Polym. Sin.* **2012**, *12*, 1482.
- 55** B. Xu, X. Wu, H. Li, H. Tong, L. Wang, *Polymer* **2012**, *53*, 490.
- 56** M. Wang, G. Zhang, D. Zhang, D. Zhu, B. Z. Tang, *J. Mater. Chem.* **2010**, *20*, 1858.
- 57** J. Liu, J. W. Y. Lam, B. Z. Tang, *Chem. Rev.* **2009**, *109*, 5799.
- 58** Y. Hong, J. W. Y. Lam, B. Z. Tang, *Chem. Soc. Rev.* **2011**, *40*, 5361.
- 59** R. Hu, E. Lager, A. Aguilar-Aguilar, J. Liu, J. W. Y. Lam, H. H. Y. Sung, I. D. Williams, Y. Zhong, K. S. Wong, E. Peña-Cabrera, B. Z. Tang, *J. Phys. Chem. C* **2009**, *113*, 15845.
- 60** P. S. Pramod, N. U. Deshpande, M. Jayakannan, *J. Phys. Chem. B* **2015**, *119*, 10511.